

# Dendrimeric siRNA for Efficient Gene Silencing\*\*

Cheol Am Hong, Ahmed A. Eltoukhy, Hyukjin Lee, Robert Langer, Daniel G. Anderson,\* and Yoon Sung Nam\*

**Abstract:** Programmable molecular self-assembly of siRNA molecules provides precisely controlled generation of dendrimeric siRNA nanostructures. The second-generation dendrimers of siRNA can be effectively complexed with a low-molecular-weight, cationic polymer (poly( $\beta$ -amino ester), PBAE) to generate stable nanostructures about 160 nm in diameter via strong electrostatic interactions. Condensation and gene silencing efficiencies increase with the increased generation of siRNA dendrimers due to a high charge density and structural flexibility.

Among the most promising nucleic acids for gene therapy is small interfering RNA (siRNA), which specifically inhibits the expression of target genes via RNA interference (RNAi) in the cytoplasm.<sup>[1]</sup> Successful siRNA therapy requires safe and efficient intracellular delivery of exogenous siRNA.<sup>[2]</sup> Cationic lipids and polyelectrolytes, which can form complexes with nucleic acids, have been widely used as gene delivery carriers because of their efficient cellular uptake and endolytic characteristics.<sup>[3]</sup> Physicochemical properties (for example size, charge, stability) of the complexes mainly depend on the electrostatic interactions between nucleic acids and the carrier materials. Plasmid DNA can be readily condensed with cationic polymers to produce stable compact nanoparticles via strong electrostatic interactions.<sup>[4]</sup> However, unlike plasmid DNA, siRNA typically does not yield condensed nanoparticles under the same conditions owing to its low charge density and its stiff molecular structure.<sup>[5]</sup>

In recent years, there has been increasing attention on the structural modification of siRNA to increase its electrostatic

condensation with conventional polymeric carriers.<sup>[6]</sup> A variety of two- and three-dimensional architectures (siRNA multimers, siRNA hydrogels, RNAi sponges) showed greatly increased cellular uptake and gene-silencing efficiency, even when low-molecular-weight cationic carriers were used.<sup>[7]</sup> However, the preparation processes involved are relatively complicated, and maintaining the quality and reproducibility of uniform siRNA nanostructures is difficult. In light of a practical path toward clinical application, it is critical to design simple, controlled, and homogenous siRNA nanostructures.

To achieve efficient siRNA delivery, the selection of a carrier material to be complexed with siRNA is also very important. We have designed, synthesized, and characterized poly( $\beta$ -amino ester)s, or PBAEs, as polymeric carriers for in vitro and in vivo gene delivery studies.<sup>[8]</sup> Syntheses and chemical modification of these polymers are relatively simple, and the polymers are hydrolytically degradable in an acidic environment as encountered in late endosomes and lysosomes.<sup>[9]</sup> Using high-throughput-combinational-library synthesis and screening methods, numerous PBAE variants have been explored to identify chemical compositions with high transfection efficiency and low cytotoxicity.<sup>[10]</sup> Although several PBAE carriers showed promising results for siRNA delivery, they required high doses of siRNA (> 125 nM) and weight ratios of PBAE to siRNA (> 100). These results suggest the importance of engineering the siRNA constructs themselves for efficient gene silencing.<sup>[11]</sup>

Dendrimeric nanostructures have been widely utilized as promising scaffolds for biomedical applications (such as gene/drug carriers and molecular probes) owing to properties including homogeneous/controlled sizes, multivalency, structural stability, and sterically crowded conformations.<sup>[12]</sup> Inspired by these unique structural properties, in this work we first demonstrate well-defined dendrimeric siRNA nanostructures with RNAi activity by programmable molecular self-assembly of chimeric DNA/siRNA strands. Dendrimeric engineering allows us to predict exactly the molecular weight, size, morphology, and number of siRNA moieties for each generation of dendrimeric siRNA. In particular, we hypothesized that a dendrimeric structure of siRNA could effectively increase the spatial charge density and structural flexibility of siRNA molecules, which could greatly affect their complexation with cationic carriers, and their gene-silencing efficiency. We used PBAE carriers previously reported for the efficient transfection of plasmid DNA but not yet for siRNA delivery.<sup>[13]</sup>

Three individual single-stranded (ss-) DNA/siRNA chimeras were mixed in stoichiometric equivalents to produce a Y-shaped siRNA molecule, ss-Y-siRNA, which served as a building block (Figure 1). The ss-oligonucleotide chimeras

[\*] Dr. C. A. Hong, Prof. Y. S. Nam  
Department of Biological Sciences, Department of Materials Science and Engineering, KI for NanoCentury (KINC CNiT)  
Korea Advanced Institute of Science and Technology  
Daejeon 305-701 (Republic of Korea)  
E-mail: yoonsung@kaist.ac.kr

Dr. A. A. Eltoukhy, Prof. R. Langer, Prof. D. G. Anderson  
Department of Biological Engineering  
The David H. Koch Institute for Integrative Cancer Research  
Massachusetts Institute of Technology  
Cambridge, MA 02139 (USA)  
E-mail: dgander@mit.edu

Prof. H. Lee  
Graduate School of Pharmaceutical Sciences, College of Pharmacy  
Ewha Womans University, Seoul (Republic of Korea)

[\*\*] This research was supported by Nano-Material Technology Development Program through the National Research Foundation of Korea (NRF) funded by the Ministry of Education, Science and Technology (2012M3A7B4049802).

Supporting information for this article is available on the WWW under <http://dx.doi.org/10.1002/anie.201412493>.

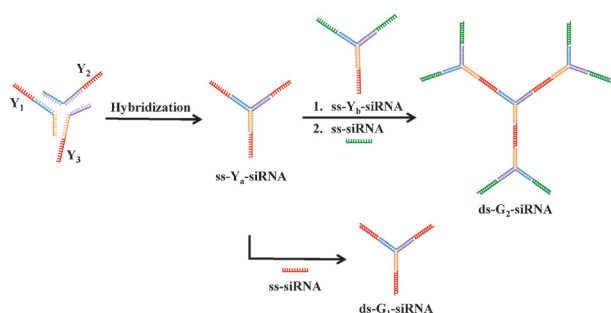


**Figure 1.** Illustration of the preparation of dendrimeric siRNA with RNAi activity via programmable molecular self-assembly.

were prepared by synthesizing 32-nucleotide (nt) DNA and 19-nt siRNA. The DNA sequences of each chimera were designed to have half-complementary base-pairing (15 nt) with two other chimeras, allowing efficient hybridization without enzymatic ligation or chemical conjugation. Self-assembled ss-Y-siRNA was composed of one three-way junction based on the DNA sequences in the core and three sticky overhangs bearing siRNA sequences in the arms. This DNA junction was composed of 45 Watson–Crick base pairs, allowing structural stability of the self-assembled siRNA in this Y-shaped conformation. Furthermore, there was a nick (2 nt) between the DNA junction and siRNA strands, which could increase the structural flexibility of dendrimeric siRNA. To achieve highly branched siRNA molecules, two kinds of ss-Y-siRNA were synthesized: ss-Y<sub>a</sub>-siRNA and ss-Y<sub>b</sub>-siRNA. Specifically, ss-Y<sub>a</sub>-siRNA was composed of three identical sequences in the arms, while ss-Y<sub>b</sub>-siRNA had one complementary arm and two different arms with ss-Y<sub>a</sub>-siRNA arms. These programmed arms can generate only one possible conformation of dendrimeric siRNA via molecular self-assembly of overhanging arms. The synthesis of the intended ss-Y-siRNA was verified using 10% polyacrylamide gel electrophoresis (PAGE) analysis (Supporting Information, Figure S1). The gel retardation of oligonucleotides mainly depends on their size, shape, and extent of base-pairing.<sup>[14]</sup> Upon mixing two individual chimeras, the PAGE assay revealed that one bright single band migrated much slower than its components, thus indicating the successful hybridization of one arm in the ss-Y-siRNA. The final products, ss-Y<sub>a</sub>-siRNA and ss-Y<sub>b</sub>-siRNA, also migrated as a single band with a greater molecular weight than partially self-assembled products of two individual chimeras. The synthetic yields of ss-Y<sub>a</sub>-siRNA and ss-Y<sub>b</sub>-siRNA were  $96.2 \pm 2.5\%$  and  $94.7 \pm 1.3\%$ , respectively, as measured by densitometry.

The well-defined dendrimeric siRNA was built from ss-Y<sub>a</sub>-siRNA molecules. Three sticky ends of ss-Y<sub>a</sub>-siRNA were hybridized with three complementary ss-siRNA to form the first-generation dendrimeric siRNA (ds-G<sub>1</sub>-siRNA). The second generation (ds-G<sub>2</sub>-siRNA) was also obtained by mixing ss-Y<sub>a</sub>-siRNA, ss-Y<sub>b</sub>-siRNA, and ss-siRNA at a ratio of 1:3:6 (molar stoichiometry) via one-pot self-assembly. The resultant ds-G<sub>2</sub>-siRNA was observed as a distinct band-shift as compared to its building blocks containing ss-Y<sub>a</sub>-siRNA, ss-Y<sub>b</sub>-siRNA, and ss-siRNA, as shown in Figure 2a. To confirm whether the annealed products were indeed ds-G<sub>2</sub>-siRNA as

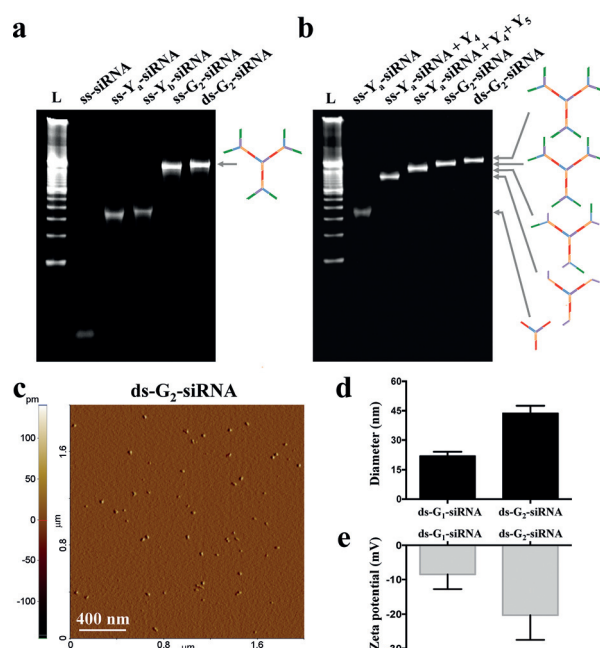


**Figure 2.** Characterization of dendrimeric siRNA nanostructures. 10% PAGE analysis for the preparation of dendrimeric siRNA via a) one-pot and b) controlled self-assembly. c) AFM image of ds-G<sub>2</sub>-siRNA. The d) hydrodynamic diameter and e) zeta potential of dendrimeric siRNA.

well as extensions from ss-Y<sub>a</sub>-siRNA, a series of rationally designed self-assembly experiments were performed. The band shifts of self-assembled products were clearly observed after increasing the hybridization of each chimeric strand from ss-Y<sub>a</sub>-siRNA to ds-G<sub>2</sub>-siRNA (Figure 2b). Notably, there was no difference in the electrophoretic mobility of the final annealing products (ds-G<sub>2</sub>-siRNA) when the gel images of control and one-pot self-assembly specimens were compared. This result indicated that dendrimeric siRNA was engineered in an extremely precise conformation according to the designed schemes via programmable molecular self-assembly. Furthermore, the size and structure of the dendrimeric siRNA could be precisely controlled in subsequent generations. During the self-assembly of ds-G<sub>2</sub>-siRNA, ss-Y<sub>a</sub>-siRNA served as an initiator core and a cross-linker, ss-Y<sub>b</sub>-siRNA extended the generation, and ss-siRNA monomers served as overhang terminators. It was notable that dendrimeric siRNA orientated the 3'-ends of siRNA in an outward manner to facilitate Dicer processing and the gene silencing effect.<sup>[15]</sup>

The morphology and size of dehydrated dendrimeric siRNA samples were examined using atomic force microscopy (AFM) in non-contact mode. Figure 2c shows that ds-G<sub>2</sub>-siRNA was formed of well-dispersed spherical nanostructures having an average diameter of  $46.64 \pm 5.72$  nm. Compared to the average diameter of native siRNA (N-siRNA, < 10 nm) in AFM images reported in our previous study,<sup>[3a]</sup> ds-G<sub>2</sub>-siRNA was much larger, suggesting successful self-assembly of the branched conformation. The average height of ds-G<sub>2</sub>-siRNA was  $1.75 \pm 0.14$  nm, which is close to the theoretical width of linear ds-oligonucleotides (ca. 2 nm).<sup>[16]</sup>

The hydrodynamic size and zeta potential of dendrimeric siRNA in an aqueous solution were determined using

dynamic light scattering (DLS). The mean diameters of ds-G<sub>1</sub>-siRNA and ds-G<sub>2</sub>-siRNA dissolved in 10 mM TE (Tris-EDTA) buffer with a pH 7.4 were  $21.9 \pm 2.1$  nm and  $43.7 \pm 3.8$  nm, respectively, which is significantly smaller than the theoretically calculated values of stretched ds-G<sub>1</sub>-siRNA (25.84 nm) and ds-G<sub>2</sub>-siRNA (61.88 nm). The results suggest that the synthesized dendrimeric siRNA molecules are self-assembled into stable three-dimensional nanostructures in an aqueous solution, which is presumably due to steric hindrance and electronic repulsion. Furthermore, the measured zeta potentials were  $-8.5 \pm 4.3$  mV and  $-20.3 \pm 8.2$  mV for ds-G<sub>1</sub>-siRNA and ds-G<sub>2</sub>-siRNA, respectively (Figure 2d and e). The well-defined dendrimeric siRNA showed much better resistance to serum-induced degradation than N-siRNA, presumably because of conformational restriction (Supporting Information, Figure S2).

To determine whether dendrimeric siRNA could readily be condensed by polymeric DNA carriers, we selected four different kinds of PBAE variants (LL24-C12-122, DD24-C12-122, DD60-C12-122, and DD90-C12-122; Supporting Information, Figure S3). These had been identified as likely useful for DNA delivery in our recent study.<sup>[13]</sup> These polymers had low-weight-average molecular weights ranging from 2.3 to 3.4 kDa (Supporting Information, Table S2), likely inadequate to formulate compact nanoparticles with short linear siRNA molecules owing to weak electrostatic interactions. We hypothesized that the structural modification of siRNA could play an important role in increasing the binding affinity for cationic carriers, ultimately contributing to the formation of compact nanoparticles by electrostatic interactions.

The dendrimeric siRNA was incubated with the PBAE variants in 25 mM sodium acetate (at pH 5.2), which has a slightly acidic pH to increase the cationization of PBAE carriers, within a range of PBAE/siRNA weight ratios (that is, 5:1, 10:1, 20:1, and 40:1). The amount of unbound siRNA molecules was investigated using a gel retardation assay. The band intensity of ds-G<sub>1</sub>-siRNA and ds-G<sub>2</sub>-siRNA gradually decreased with increasing weight ratios for all PBAEs tested (Figure 3a). This decrease in band intensity was markedly lower for the complexed dendrimeric siRNA compared to N-siRNA under the same conditions. At a weight ratio of 40:1, no significant amount of unbound siRNA was observed in ds-G<sub>1</sub>-siRNA/PBAE and ds-G<sub>2</sub>-siRNA/PBAE complexes, suggesting the successful incorporation of siRNA into PBAEs by electrostatic interactions. Notably, the binding efficiency of ds-G<sub>2</sub>-siRNA to PBAEs was much higher than that of ds-G<sub>1</sub>-siRNA. These results indicate that the degree of branching in dendrimeric siRNA significantly affected the efficiency of condensation with cationic polymer carriers.

To further investigate the polymeric condensation, the sizes and zeta potentials of various siRNA/PBAE complexes were measured using DLS at a weight ratio of 40:1 (Figure 3b and c). For all of the PBAEs tested in this work, the diameters of ds-G<sub>1</sub>-siRNA/PBAE and ds-G<sub>2</sub>-siRNA/PBAE complexes were in the ranges of 220–280 nm and 160–270 nm, respectively. These particle sizes are generally considered compact enough to permit efficient cellular uptake by endocytosis.<sup>[17]</sup> In contrast, the N-siRNA/PBAE complexes showed compa-

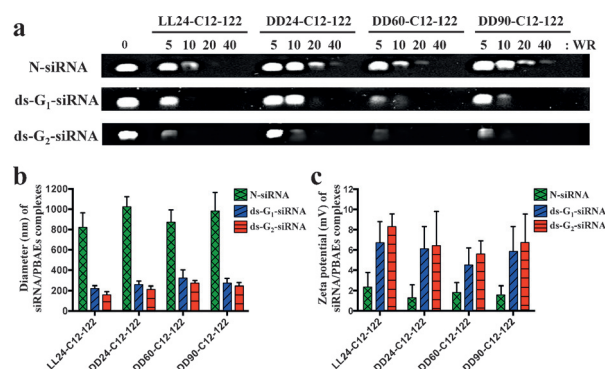


**Figure 3.** Physicochemical properties of dendrimeric siRNA/PBAE complexes. a) 1% agarose gel images for confirmation of siRNA binding affinity upon contact with PBAE carriers at different weight ratios (WR) of carriers to siRNA. The b) hydrodynamic diameters and c) zeta potentials of dendrimeric siRNA/PBAE complexes.

ratively large particle diameters ( $> 820$  nm). The zeta potentials of ds-G<sub>1</sub>-siRNA/PBAE complexes ( $+4.5$ – $6.7$  mV) and ds-G<sub>2</sub>-siRNA/PBAE complexes ( $+5.6$ – $8.3$  mV) showed a higher positive surface charge than N-siRNA/PBAE complexes ( $+1.2$ – $2.3$  mV) for all PBAEs tested. As expected, ds-G<sub>2</sub>-siRNA/PBAE complexes had smaller diameters and higher zeta potentials than ds-G<sub>1</sub>-siRNA/PBAE complexes.

To verify target-specific gene silencing capability, two different sequences of green fluorescent protein (GFP)-siRNA were employed. Three arms of ds-G<sub>1</sub>-siRNA were designed with identical siRNA sequences that targeted 1093–1112 of GFP mRNA, while ds-G<sub>2</sub>-siRNA had two different target sites (1093–1112 and 1204–1233) owing to the controlled extension form ds-G<sub>1</sub>-siRNA. Thus, while ds-G<sub>1</sub>-siRNA incorporated three copies of identical siRNA (red, Figure 1), ds-G<sub>2</sub>-siRNA had nine copies of two different siRNAs, comprising three copies (red, Figure 1) and six copies (green, Figure 1) of siRNA. These target locations on the GFP-mRNA were successfully used as GFP-siRNA sequences for RNAi activity in our previous study.<sup>[18]</sup> This approach enables the simultaneous silencing of multiple target genes in a single step, as a new strategy for combinatorial RNAi technology. Using fluorescence-activated cell sorting (FACS) analysis, the gene silencing efficiency was investigated following treatment of GFP-overexpressing KB (GFP-KB) cells with various siRNA/PBAE complexes in media containing 10% serum (Figure 4a). The concentration of siRNA in dendrimeric siRNA was exactly calculated using the number of siRNA motifs. The N-siRNA/PBAE complexes did not show any significant GFP suppression at an siRNA concentration of 25 nM. Furthermore, ss-G<sub>1</sub>-siRNA/PBAE complexes exhibited negligible gene silencing (Supporting Information, Figure S4). However, complexes containing ds-G<sub>1</sub>-siRNA and ds-G<sub>2</sub>-siRNA efficiently inhibited GFP expression. The level of GFP expression in cells treated with ds-G<sub>1</sub>-siRNA/PBAE complexes decreased to  $34.5 \pm 1.9\%$  when using the LL24-C12-122 PBAE variant,  $48.9 \pm 2.2\%$  when using DD24-C12-122,  $75.1 \pm 3.0\%$  when using DD60-C24-122, and  $57.1 \pm 1.6\%$  when using DD90-C24-122. For complexes containing ds-G<sub>2</sub>-siRNA/PBAE, these levels were  $27.2 \pm 1.9\%$  using LL24-C12-122,  $45.1 \pm 1.5\%$  using DD24-



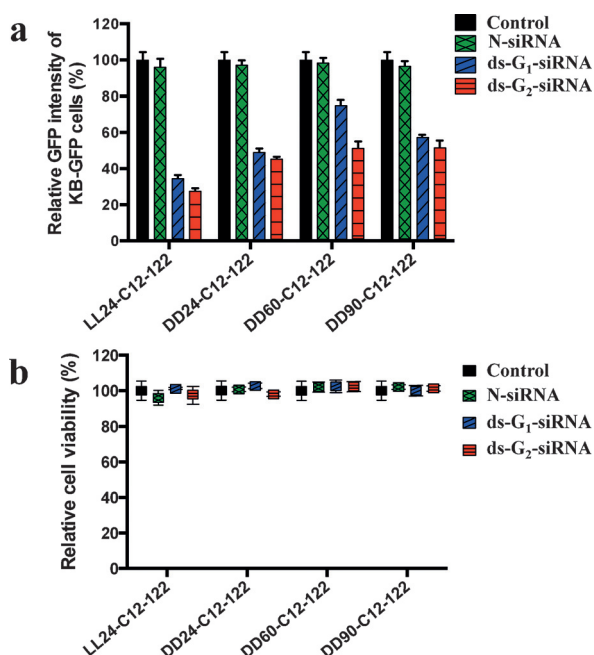


**Figure 4.** Gene silencing efficiency of dendrimeric siRNA. a) Target-gene silencing effect and b) cell viability of GFP-KB cells treated with various siRNA/PBAE complexes in a 10% serum-containing medium.

C24-122,  $50.9 \pm 4.1\%$  using DD60-C24-122, and  $51.1 \pm 4.9\%$  using DD90-C24-122. Furthermore, the complexes containing ss-G<sub>2</sub>-siRNA showed a noticeable inhibition of GFP expression, indicating the biological activity of ds-G<sub>1</sub>-siRNA within ds-G<sub>2</sub>-siRNA for the RNAi pathway as shown in the Supporting Information, Figure S4.

Notably, ds-G<sub>2</sub>-siRNA showed a relatively higher gene silencing efficiency than ds-G<sub>1</sub>-siRNA under the same conditions, though gene silencing efficiency depends on the type of polymeric carriers. Furthermore, gene silencing is not proportional to the number of siRNA per structure because siRNA can repeatedly cleave target mRNA due to the recirculation of RNA-inducing silencing complex (RISC).<sup>[2b]</sup> Endogenous enzyme (Dicer) processing is prerequisite to gene silencing of DNA/siRNA hybrid nanostructures.<sup>[7c]</sup> It is thus a reasonable presumption that the outer-branched form of ds-G<sub>2</sub>-siRNA is equal to that of ds-G<sub>1</sub>-siRNA because Dicer can cleave the outer siRNA (green) in the same manner as it does for ds-G<sub>1</sub>-siRNA (red). Furthermore, gene silencing was observed in the cells treated with ss-G<sub>2</sub>-siRNA complexes (Supporting Information, Figure S4), resulting in the specific cleavage of inner siRNA (red) within G<sub>2</sub>-siRNA by Dicer. Accordingly, ds-G<sub>2</sub>-siRNA can be degraded to release smaller DNA/siRNA fragments with two arms, which well demonstrated as Dicer substrates for gene silencing.<sup>[19,15a]</sup> Again, in our experimental design, it is difficult to clearly show a dramatic difference of gene silencing efficiency between ss-G<sub>2</sub>-siRNA and ds-G<sub>2</sub>-siRNA complexes (Supporting Information, Figure S4). Different siRNA targets must be used to fully demonstrate the gene silencing activity of individual siRNA with G<sub>2</sub>-siRNA. Despite this limitation in the current design, all of our gene silencing data showed that ds-G<sub>2</sub>-siRNA complexes were more effective than ds-G<sub>1</sub>-siRNA

complexes (Figure 3). We suggest that the higher spatial charge density and structural flexibility of ds-G<sub>2</sub>-siRNA compared with ds-G<sub>1</sub>-siRNA allow more effective interactions with PBAEs that enable formation of more stable nanoparticles. This facilitates cellular uptake of siRNA, followed by more efficient gene silencing.

Along with a reduced proportion of GFP-KB cells, we also observed a strong shift in fluorescence intensity in GFP-KB cells transfected by ds-G<sub>1</sub>-siRNA/PBAE and ds-G<sub>2</sub>-siRNA/PBAE complexes at an siRNA concentration of 50 nM. This shift in fluorescence intensity was greater than that of cells treated with N-siRNA/PBAE complexes (Supporting Information, Figure S5). Based on the flow cytometry results, the use of dendrimeric siRNA was clearly associated with substantial reduction of GFP expression in GFP-KB cells. The cell viabilities of N-siRNA, ds-G<sub>1</sub>-siRNA, and ds-G<sub>2</sub>-siRNA complexes formulated using various PBAEs were examined using a CCK-8 assay. Figure 4b shows that there was no significant reduction in viability of cells treated with dendrimeric siRNA/PBAE complexes at a polymer-to-siRNA weight ratio of 40:1 and an siRNA dose of 100 nM. This result indicates that the silencing of the target genes could be attributed to the RNAi effect. It is interesting to note that dendrimeric siRNA complexes prepared with linear polyethylenimines (LPEIs, 2.5 kDa and 25 kDa) and branched polyethylenimine (BPEI, 25 kDa) showed a much higher gene silencing effect than N-siRNA complexes (Supporting Information, Figure S6).

In conclusion, we report the first attempt to design and fabricate dendrimeric siRNA for enhanced complexation with degradable polymeric carriers, resulting in efficacious cellular uptake and gene silencing. The programmable self-assembly strategy for oligonucleotides was successfully applied to achieve precise control of the generation of dendrimeric siRNA nanostructures. Most importantly, dendrimeric siRNA was effectively condensed to generate compact, stable complexes on contact with optimized DNA carriers of PBAE due to the increased charge density and structural flexibility of dendrimeric siRNA. The resulting dendrimeric siRNA/PBAE complexes showed a significant inhibition of target-gene expression in cells, as compared to that of native siRNA/PBAE complexes. Therefore, engineered siRNA nanostructures could potentially be utilized as new platforms to improve polymeric condensation of nanoparticles for polymer-based siRNA delivery systems.

**Keywords:** dendrimeric nanostructures · gene silencing · poly( $\beta$ -amino ester) · polymeric condensation · siRNA

**How to cite:** *Angew. Chem. Int. Ed.* **2015**, *54*, 6740–6744  
*Angew. Chem.* **2015**, *127*, 6844–6848

- a) D. Castanotto, J. J. Rossi, *Nature* **2009**, *457*, 426–433; b) R. Kanasty, J. R. Dorkin, A. Vegas, D. Anderson, *Nat. Mater.* **2013**, *12*, 967–977; c) S. M. Elbashir, J. Harborth, W. Lendeckel, A. Yalcin, K. Weber, T. Tuschl, *Nature* **2001**, *411*, 494–498.
- a) R. L. Kanasty, K. A. Whitehead, A. J. Vegas, D. G. Anderson, *Mol. Ther.* **2012**, *20*, 513–524; b) M. Dominska, D. M. Dykxhoorn, *J. Cell Sci.* **2010**, *123*, 1183–1189.

- [3] a) C. A. Hong, J. S. Kim, S. H. Lee, W. H. Kong, T. G. Park, H. Mok, Y. S. Nam, *Adv. Funct. Mater.* **2013**, 23, 316–322; b) J. Yang, W. Hendricks, G. Liu, J. M. McCaffery, K. W. Kinzler, D. L. Huso, B. Vogelstein, S. Zhou, *Proc. Natl. Acad. Sci. USA* **2013**, 110, 14717–14722.
- [4] a) M. Ikonen, L. Murtomäki, K. Kontturi, *Colloids Surf. B* **2008**, 66, 77–83; b) M. X. Tang, F. C. Szoka, *Gene Ther.* **1997**, 4, 823–832.
- [5] a) C. Scholz, E. Wagner, *J. Controlled Release* **2012**, 161, 554–565; b) P. Kebbekus, D. E. Draper, P. Hagerman, *Biochemistry* **1995**, 34, 4354–4357; c) P. J. Hagerman, *Biopolymers* **1981**, 20, 1503–1535; d) P. J. Hagerman, *Annu. Rev. Biophys. Biophys. Chem.* **1988**, 17, 265–286.
- [6] a) S. J. Lee, S. Son, J. Y. Yhee, K. Choi, I. C. Kwon, S. H. Kim, K. Kim, *Biotechnol. Adv.* **2013**, 31, 491–450; b) S. H. Lee, B. H. Chung, T. G. Park, Y. S. Nam, H. Mok, *Acc. Chem. Res.* **2012**, 45, 1014–1025.
- [7] a) H. Mok, S. H. Lee, J. W. Park, T. G. Park, *Nat. Mater.* **2010**, 9, 272–278; b) C. A. Hong, S. H. Lee, J. S. Kim, J. W. Park, K. H. Bae, H. Mok, T. G. Park, H. Lee, *J. Am. Chem. Soc.* **2011**, 133, 13914–13917; c) J. B. Lee, J. Hong, D. K. Bonner, Z. Poon, P. T. Hammond, *Nat. Mater.* **2012**, 11, 316–322.
- [8] a) D. Lynn, D. Anderson, D. Putnam, R. Langer, *J. Am. Chem. Soc.* **2001**, 123, 8155–8156; b) D. G. Anderson, D. M. Lynn, R. Langer, *Angew. Chem. Int. Ed.* **2003**, 42, 3153–3158; *Angew. Chem.* **2003**, 115, 3261–3266; c) D. G. Anderson, A. Akinc, N. Hossain, R. Langer, *Mol. Ther.* **2005**, 11, 426–438.
- [9] a) S. Y. Tzeng, B. P. Hung, W. L. Grayson, J. J. Green, *Biomaterials* **2012**, 33, 8142–8151; b) K. L. Kozielski, S. Y. Tzenga, J. J. Green, *Chem. Commun.* **2013**, 49, 5319–5321.
- [10] a) M. Keeney, S. Ong, A. Padilla, Z. Yao, S. Goodman, J. C. Wu, F. Yang, *ACS Nano* **2013**, 7, 7241–7250; b) J. J. Green, G. T. Zugates, R. Langer, D. G. Anderson, *Methods Mol. Biol.* **2009**, 480, 53–63; c) J. J. Green, R. Langer, D. G. Anderson, *Acc. Chem. Res.* **2008**, 41, 749–759; d) A. A. Eltoukhy, D. J. Siegwart, C. A. Alabi, J. S. Rajan, R. Langer, D. G. Anderson, *Biomaterials* **2012**, 33, 3594–3603.
- [11] a) D. Jere, C. X. Xu, R. Arote, C. H. Yun, M. H. Cho, C. S. Cho, *Biomaterials* **2008**, 29, 2535–2547; b) R. E. Vandenbroucke, B. G. De Geest, S. Bonne, M. Vinken, T. Van Haecke, H. Heimberg et al., *J. Gene Med.* **2008**, 10, 783–794; c) J. S. Lee, J. J. Green, K. T. Love, J. Sunshine, R. Langer, D. G. Anderson, *Nano Lett.* **2009**, 9, 2402–2406.
- [12] a) T. Yu, L. Xiaoxuan, B. Anne-Laure, W. Yang, L. Cheng, E. Patrick Erbacher, Q. Fanqi, R. Palma, B. J.-P. Behr, P. Ling, *Angew. Chem. Int. Ed.* **2012**, 51, 8478–8484; *Angew. Chem.* **2012**, 124, 8606–8612; b) J. F. Kukowska-Latallo, A. U. Bielinska, J. Johnson, R. Spindler, D. A. Tomalia, J. R. Bake, *Proc. Natl. Acad. Sci. USA* **1996**, 93, 4897–4802.
- [13] A. A. Eltoukhy, D. Chen, C. A. Alabi, R. Langer, D. G. Anderson, *Adv. Mater.* **2013**, 25, 1487–1493.
- [14] Y. Li, Y. D. Tseng, S. Y. Kwon, L. d’Espaux, J. S. Bunch, P. L. McEuen, D. Luo, *Nat. Mater.* **2004**, 3, 38–42.
- [15] a) C. I. Chang et al., *J. Gene Med.* **2012**, 14, 138–146; b) C. I. Chang, S. W. Hong, S. Kim, D. K. Lee, *Biochem. Biophys. Res. Commun.* **2007**, 359, 997–1003.
- [16] a) C. A. Hong, B. Jang, E. H. Jeong, H. Jeong, H. Lee, *Chem. Commun.* **2014**, 50, 13049–13051; b) J. Adamcik, D. V. Klinov, G. Witz, S. K. Sekatskii, G. Dietler, *FEBS Lett.* **2006**, 580, 5671.
- [17] a) S. Zhang, S. J. Li, G. Lykotrafitis, G. Bao, S. Suresh, *Adv. Mater.* **2009**, 21, 419–424; b) C. H. Choi, L. Hao, S. P. Narayan, E. Auyeung, C. A. Mirkin, *Proc. Natl. Acad. Sci. USA* **2013**, 110, 7625–7630; c) S. J. Lee et al., *Mol. Ther.* **2014**, 22, 397–408.
- [18] a) S. D. Jo, J. S. Kim, C. C. Joe, H. Mok, Y. S. Nam, *Macromol. Biosci.* **2014**, 14, 195–201; b) H. Lee et al., *Nat. Nanotechnol.* **2012**, 7, 389–393.
- [19] a) S. Sajeesh et al., *J. Controlled Release* **2014**, 196, 28–36.

Received: December 31, 2014

Revised: February 9, 2015

Published online: April 17, 2015